AIAA JOURNAL
Vol. 36, No. 8, August 1998

Dynamic Response of Initially Loaded Piezoelectric Plates Composed of Short Fibers

Wen-Shyong Kuo*
Feng Chia University, Taichung 407, Taiwan, Republic of China

The vibration behavior of piezoelectric plates under initial electromechanical loads is examined. A unified micromechanics approach is adopted for determining the effective electroelastic properties of composites composed of short fibers. The fibers are treated as spheroidal inclusions. Both the matrix and inclusions are assumed to be linearly piezoelastic and transversely isotropic. The electroelastic Eshelby tensors for ellipsoidal inclusions have been obtained and also evaluated numerically for finite fiber aspect ratios. Utilizing these tensors and applying the Mori–Tanaka mean field theory to account for the interaction between inclusions and matrix, the effective electroelastic properties of the composites are obtained. These properties are then used to evaluate the vibration behavior of the plates subjected to preexisting electromechanical loads. The Trefftz equations and the variational principle are used to account for initial stresses. Numerical examples are given for the $BaTiO_3$/PZT-5H and carbon/PZT-5H composites. The effects of piezoelastic coupling on the elastic moduli and fundamental frequency have been assessed. It is found that piezoelastic coupling provides a stiffening effect on the material, thus increasing the fundamental frequency of the plate. The influence of piezoelastic coupling is more pronounced when shorter fibers are used. The coupling effects vanish when the material becomes monolithic. Similar to applied mechanical loads, initial electric fields also affect the dynamic response of the plate, and plate buckling can occur when the applied initial electromechanical loads reach critical values.

Introduction

RESEARCH and development activities in piezoelectric materials are now intense and widespread. Practical applications are numerous and spread across many industries. In processing of piezoelectric materials, initial electromechanical stresses often occur, especially when two distinct constituents are involved in the materials. Residual electric field, thermal expansion mismatch, and phase transformation might represent typical sources for the cause of initial electromechanical stresses, which could be critical in affecting the performance of the composites. For better material utilization, the influence of the stresses on a piezoelectric composite is of interest to pursue. This paper is aimed at the vibration behavior of composite plates composed of short fibers, and the initial loads examined include in-plane normal stresses, a twisting shear acting on the edges, and an electric field.

The electroelastic constants of the composite should be evaluated before examining its dynamic response. For predicting the material properties of short-fiber composites, several approaches have been proposed. The simplest is probably the so-called aggregate model,[1–3] which applies the known properties of constituents to the evaluation of the overall composite properties through a virtual rule-of-mixtures approach. This model is known to be more suitable for properties associated with the fiber direction. Because this macroscopic approach is established on a volume basis, the geometric aspects of reinforcing fibers and the interactions between fibers and matrix are ignored. The shear-lag method is perhaps the easiest to account for fiber length effects.[4,5] This method assumes that the interfacial shear stress is proportional to the displacement difference between the fiber and matrix. With this assumption, the distribution of normal stress along the axial direction of the fiber can be obtained. No information regarding the stress and strain fields normal to the fiber can be obtained by this method. Because both methods are highly simplified, they are unsuitable for the present study in which the fiber length is critical. More importantly, although both methods are intended to describe the relation between deformation and force, they are inappropriate to be the tools for the resulting electric properties, which are prerequisites to the analysis of piezoelastic composites. For this reason, a more complex micromechanics approach able to provide information on the fiber length and resulting electroelastic properties is required.

Micromechanics, treating fibers as spheroidal inclusions and focusing on the interactions between inclusions and the surrounding matrix, is generally believed to be the most powerful tool in handling short-fiber-reinforced composites, although the mathematical formulation is generally complex. For a composite containing a finite concentration of inclusions, the Mori–Tanaka mean field theory is used to study the overall behavior. Based on the equivalent inclusion method,[6] Mori and Tanaka[7] and Mura[8] first introduced the concept of average stress in a matrix material containing precipitates with eigenstrain. This theory has been successfully applied to study the elastic behavior and effective properties of short-fiber composites.[9–12] In this work, the same concept is adopted to model short-fiber piezoelectric composites and to assess the influence of fiber length and fiber content on the resulting electroelastic behavior. The bondings between fibers and the matrix are assumed to be perfect, and the matrix is assumed to be void free. From a practical point of view, most piezoelectric materials are transversely isotropic, and hence the constituents in this study are limited to be transversely isotropic, although handling anisotropic cases involves essentially the same effort.

By modeling the disturbed strain and electric field induced by an electromechanical load as eigenfields, the anisotropic inclusion method is first extended to consider the inherently anisotropic and coupled behavior of a piezoelectric composite. Then the coupled electroelastic Eshelby tensors that govern the strain and electric displacement of a piezoelectric spheroidal inclusion are numerically obtained. Finally, based on the Mori–Tanaka mean field theory, the effective electroelastic moduli of two-phase piezoelectric composite materials are obtained analytically, and the piezoelastic coupling effect is examined.

Electroelastic Eshelby Tensors

Consider a sufficiently large piezoelectric composite $\boldsymbol{D}$ with elastic constants C_{ijmn}, piezoelectric constants e_{imn}, and dielectric constants κ_{in}, which tends to undergo eigenstrain (or stress-free transformation strain) ε^*_{ab} and eigenelectric field (or electric displacement-free transformation electric field) E^*_b in a spheroidal inclusion having semiaxes a_1 and a_3 as shown in Fig. 1. Varying the aspect ratio of the spheroidal inclusion enables the modeling of

Received March 18, 1997; revision received April 1, 1998; accepted for publication April 13, 1998.

*Associate Professor, Department of Textile Engineering.

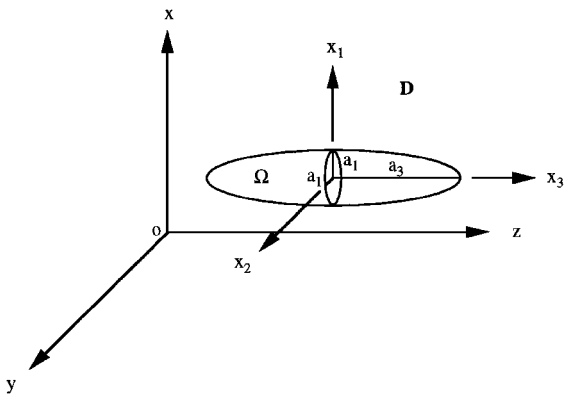

Fig. 1 Spheroidal inclusion.

fibers ranging from penny shape to continuous filament. Suppose that the crystalline directions of the matrix coincide with the principal axes of the inclusion and that both the piezoelectric matrix and the piezoelectric inclusion are transversely isotropic with x_3 being the symmetric axis. The piezoelastic constitutive equations that coupled the deformation and electric fields are given as[11,12]

$$\sigma_{ij} = C_{ijmn}\varepsilon_{mn} - e_{nij}E_n, \qquad D_i = e_{imn}\varepsilon_{mn} + \kappa_{in}E_n \tag{1}$$

When the eigenstrain ε^*_{ab} and the eigenelectric field E^*_b in the inclusion are uniform, the induced strain ε_{mn} and electric field E_n inside Ω can be expressed as

$$\varepsilon_{mn} = S_{mnab}\varepsilon^*_{ab} - S_{mn4b}E^*_b, \qquad E_n = S_{4n4b}E^*_b - S_{4nab}\varepsilon^*_{ab} \tag{2}$$

where S_{MnAb} is referred to as the electroelastic Eshelby tensor. Herein, the lowercase subscripts range from 1 to 3, whereas the uppercase subscripts range from 1 to 4; the subscript 4 is associated with piezoelectric quantities. The Eshelby tensors have been obtained previously.[12]

When the strain and electric fields are known, the corresponding stress σ_{ij} and electric displacement D_i inside the inclusion due to a uniform eigenfield are given by

$$\begin{aligned}\sigma_{ij} &= C_{ijmn}\left(S_{mnab}\varepsilon^*_{ab} - S_{mn4b}E^*_b - \varepsilon^*_{mn}\right)\\ &\quad - e_{nij}\left(S_{4n4b}E^*_b - S_{4nab}\varepsilon^*_{ab} - E^*_n\right)\\ D_i &= e_{imn}\left(S_{mnab}\varepsilon^*_{ab} - S_{mn4b}E^*_b - \varepsilon^*_{mn}\right)\\ &\quad + \kappa_{in}\left(S_{4n4b}E^*_b - S_{4nab}\varepsilon^*_{ab} - E^*_n\right)\end{aligned} \tag{3}$$

where the nonzero elements in C_{ijmn}, e_{nij}, and κ_{in} for a transversely isotropic material can be expressed in the Voight two-index notation as[12]

$$[\boldsymbol{C}] = \begin{bmatrix} C_{11} & C_{12} & C_{13} & 0 & 0 & 0\\ & C_{11} & C_{13} & 0 & 0 & 0\\ & & C_{33} & 0 & 0 & 0\\ & & & C_{44} & 0 & 0\\ & \text{sym.} & & & C_{44} & 0\\ & & & & & C_{66}\end{bmatrix} \tag{4}$$

$$[\boldsymbol{e}] = \begin{bmatrix} 0 & 0 & 0 & 0 & e_{15} & 0\\ 0 & 0 & 0 & e_{15} & 0 & 0\\ e_{31} & e_{31} & e_{33} & 0 & 0 & 0\end{bmatrix} \tag{5}$$

$$[\kappa] = \begin{bmatrix} \kappa_{11} & 0 & 0\\ 0 & \kappa_{11} & 0\\ 0 & 0 & \kappa_{33}\end{bmatrix} \tag{6}$$

where $C_{66} = (C_{11} - C_{12})/2$.

The Eshelby tensor in Eqs. (2) and (3) can be expressed in the following forms:

$$\begin{aligned} S_{mnab} &= (1/8\pi)[C_{ijab}(G_{mjin} + G_{njim}) - e_{iab}(G_{m4in} + G_{n4im})]\\ S_{mn4b} &= (1/8\pi)[e_{bij}(G_{mjin} + G_{njim}) + \kappa_{ib}(G_{m4in} + G_{n4im})]\\ S_{4nab} &= (1/4\pi)(C_{ijab}G_{4jin} - e_{iab}G_{44in})\\ S_{4n4b} &= (1/4\pi)(e_{bij}G_{4jin} + \kappa_{ib}G_{44in})\end{aligned} \tag{7}$$

The expression G_{MJin} in Eq. (7) is given by

$$\begin{aligned} G_{MJin} &= \int_{-1}^{1}\int_{0}^{2\pi} N_{MJ}(\zeta)D^{-1}(\zeta)\zeta_i\zeta_n \,\mathrm{d}\beta\,\mathrm{d}\zeta_3\\ \zeta_1 &= \sqrt{1-\zeta_3^2}\cos(\beta), \qquad \zeta_2 = \sqrt{1-\zeta_3^2}\sin(\beta)\end{aligned} \tag{8}$$

where $N_{MJ}(\zeta)$ and $D(\zeta)$ are the cofactor and determinant of the 4×4 matrix $C_{iMJn}\zeta_i\zeta_n$, respectively. Here C_{iMJn} is the generalized stiffness matrix defined as

$$C_{iJMn} = \begin{cases} C_{ijmn} & J \le 3;\ M \le 3\\ e_{nij} & J \le 3;\ M = 4\\ e_{imn} & J = 4;\ M \le 3\\ -\kappa_{in} & J = 4;\ M = 4\end{cases} \tag{9}$$

Provided that all material constants are given, the double integration in Eq. (8) can be carried out numerically, and thus the Eshelby tensor can be obtained from Eq. (9). It is found that only 15 elements in the electroelastic tensor are independent and can be divided into two groups. The first group includes S_{1111}, S_{1122}, S_{1133}, S_{1313}, S_{1212}, S_{4141}, and S_{1143}; and the second group includes S_{3333}, S_{3311}, S_{1341}, S_{3343}, S_{4113}, S_{4311}, S_{4333}, and S_{4343}. When the inclusion aspect ratio a_3/a_1 tends to infinity, i.e., continuous fiber, the elements in the second group vanish, whereas those in the first group reduce to the following closed-form solutions:

$$\begin{aligned} S_{1111} &= \frac{5C_{11} + C_{12}}{8C_{11}}, \qquad S_{1122} = \frac{3C_{12} - C_{11}}{8C_{11}}\\ S_{1133} &= \frac{C_{13}}{2C_{11}}, \qquad S_{1313} = \frac{1}{4}, \qquad S_{1212} = \frac{3C_{11} - C_{12}}{8C_{11}}\\ S_{4141} &= \frac{1}{2}, \qquad S_{1143} = \frac{e_{31}}{2C_{11}}\end{aligned} \tag{10}$$

Effective Electroelastic Moduli

Consider a sufficiently large two-phase piezoelectric composite $\boldsymbol{D}$ composed of ellipsoidal inclusions Ω embedded in a piezoelectric matrix. The electroelastic constants for the inclusions and the matrix are denoted C^*_{iJMn} and C_{iJMn}, respectively. To evaluate the effective electroelastic moduli of the composite, the Mori–Tanaka mean field theory, which is believed to be one of the most powerful tools in this issue, is used. This theory generally yields identical results when either a traction-electric displacement or an elastic displacement-electric field is prescribed on the boundary of the composite. In this paper, the former is adopted.

When subjected to a far-field traction and electric displacement on the boundary, the induced strain in the absence of inclusions is denoted as ε^0_{Mn}. Then the presence of an inclusion provides disturbance in local fields of the inclusion. The volume average of the disturbed stress and electric field must vanish:

$$(1-f)\left\langle\sigma^m_{iJ}\right\rangle + f\left\langle\sigma^{\Omega}_{iJ}\right\rangle = 0 \tag{11}$$

where the angle bracket $\langle\rangle$ represents the volume averaging over the entire composite domain and f is the volume fraction of inclusions. The generalized stress and strain are defined to include electric terms as

$$\sigma_{iJ} = \begin{cases}\sigma_{ij} & J \le 3\\ D_i & J = 4\end{cases}, \qquad \varepsilon_{iJ} = \begin{cases}\varepsilon_{ij} & J \le 3\\ -E_i & J = 4\end{cases} \tag{12}$$

The average disturbed stress and electric displacement in the matrix and the kth inclusion can be expressed as

$$\begin{aligned} \langle \sigma_{iJ}^{m} \rangle &= C_{iJMn} \langle \varepsilon_{Mn}^{m} \rangle \qquad \text{in} \qquad \boldsymbol{D} - \Omega \\ \langle \sigma_{iJ}^{\Omega k} \rangle &= C_{iJMn}^{*} \left(\langle \varepsilon_{Mn}^{m} \rangle + \langle \varepsilon_{Mn} \rangle \right) \qquad \text{in} \qquad \Omega_k \end{aligned} \tag{13}$$

where $\langle \varepsilon_{Mn}^{m} \rangle$ is the average generalized strain and $\langle \varepsilon_{Mn} \rangle$ is the average disturbance strain in the inclusion Ω_k. Because all inclusions are assumed to have the same geometric shapes and material properties, the average value over Ω_k is identical with that over other inclusions, namely, $\langle \sigma_{iJ}^{\Omega k} \rangle = \langle \sigma_{iJ}^{\Omega} \rangle$.

When subjected to a uniform load σ_{Mn}^{0} at the far field, the average generalized stress in inclusions can be expressed as

$$\sigma_{Mn}^{0} + \langle \sigma_{iJ}^{\Omega} \rangle = C_{iJMn}^{*} \left(\langle \varepsilon_{Mn}^{0} \rangle + \langle \varepsilon_{Mn}^{m} \rangle + \varepsilon_{Mn} \right) \tag{14}$$

In Eq. (13), the relation $\langle \varepsilon_{Mn} \rangle = \varepsilon_{Mn}$ in Ω has been used because the applied electromechanical load is uniform and the inclusion is ellipsoidal.

According to the equivalent inclusion method,[6] the stress and electric displacement in inclusions can be simulated by those in an equivalent inclusion with the electroelastic constants of the matrix and a fictitious eigenstrain and eigenelectric field ε_{Mn}^{*}. Therefore, Eq. (14) can be written as

$$\sigma_{Mn}^{0} + \langle \sigma_{iJ}^{\Omega} \rangle = C_{iJMn} \left(\langle \varepsilon_{Mn}^{0} \rangle + \langle \varepsilon_{Mn}^{m} \rangle + \varepsilon_{Mn} - \varepsilon_{Mn}^{*} \right) \tag{15}$$

where the disturbed field ε_{Mn} can be related to the fictitious eigenfield by

$$\varepsilon_{Mn} = S_{MnAb} \varepsilon_{Ab}^{*} \tag{16}$$

By substituting Eq. (16) into Eq. (15), one can obtain the average generalized stress in inclusions as

$$\langle \sigma_{iJ}^{\Omega} \rangle = C_{iJMn} \langle \varepsilon_{Mn}^{m} \rangle + C_{iJMn} (S_{MnAb} - I_{MnAb}) \varepsilon_{Mn}^{*} \tag{17}$$

where I_{MnAb} is the fourth-order identity tensor defined as

$$I_{MnAb} = \begin{cases} (\delta_{ma}\delta_{ma} + \delta_{ma}\delta_{ma})/2 & M \le 3;\ A \le 3 \\ \delta_{nb} & M = 4;\ A = 4 \\ 0 & \text{otherwise} \end{cases} \tag{18}$$

Combining Eqs. (12), (13), and (19) leads to

$$\langle \varepsilon_{Mn}^{m} \rangle = -f (S_{MnAb} - I_{MnAb}) \varepsilon_{Mn}^{*} \tag{19}$$

Substituting this relation into Eqs. (14) and (17) yields

$$\langle \sigma_{iJ}^{m} \rangle = -f C_{iJMn} (S_{MnAb} - I_{MnAb}) \varepsilon_{Mn}^{*} \tag{20}$$

$$\langle \sigma_{iJ}^{\Omega} \rangle = (1 - f) C_{iJMn} (S_{MnAb} - I_{MnAb}) \varepsilon_{Mn}^{*} \tag{21}$$

The equivalent eigenstrain can be solved from Eqs. (15) and (19) as

$$\varepsilon_{Mn}^{*} = -U_{AbiJ}^{-1} \left(C_{iJMn}^{*} - C_{iJMn} \right) \varepsilon_{Mn}^{0} \tag{22}$$

where U_{AbiJ}^{-1} is the inverse of U_{iJAb} given by

$$U_{AbiJ} = \left(C_{iJMn}^{*} - C_{iJMn} \right) [(1 - f) S_{MnAb} + f I_{MnAb}] + C_{iJMn} \tag{23}$$

The overall strain of the composite is the sum of the average strains in the matrix and inclusions weighted by their volume fractions. Based on this, the average composite strain can be obtained as

$$\langle \varepsilon_{Mn}^{c} \rangle = \varepsilon_{Mn}^{0} + f \varepsilon_{Mn}^{*} \tag{24}$$

Because the equivalent eigenstrain has been obtained in Eq. (22), the average composite strain can be expressed as

$$\langle \varepsilon_{Mn}^{c} \rangle = L_{MniJ}^{c} \sigma_{iJ}^{0} \tag{25}$$

where L_{MniJ}^{c} is the effective composite compliance defined as

$$L_{MniJ}^{c} = \left[I_{MnAb} - f U_{MnqR}^{-1} \left(C_{qRAb}^{*} - C_{qRAb} \right) \right] C_{AbiJ}^{-1} \tag{26}$$

The effective composite stiffness C_{iJAb}^{c} can be obtained by the inverse of the compliance.

Evaluations of U_{MnqR}^{-1} from Eq. (23) and C_{iJAb}^{c} from Eq. (26) involve inversions of fourth-order tensors. However, there is a lack of a standard mathematical operation for the tensor inversion. For this reason, a special scheme has been developed. First, the fourth-order compliance tensor is used to map to a Voight two-index 9×9 compliance matrix with indices 1–6 representing elastic terms and 7–9 representing electric terms. This matrix can then be inverted readily to obtain the associated 9×9 stiffness matrix. Finally, this stiffness matrix is used to map and to generate the resulting fourth-order stiffness tensor.

Plate Under Initial Stresses

This section examines the governing equation of motion for the piezoelectric composite under initial electromechanical stresses. In dealing with the motion of the composite, the material is assumed to be uniform macroscopically with the electroelastic constants obtained from Eq. (26). According to Bolotin,[13] the equilibrium equation and boundary traction condition can be expressed in terms of Trefftz stress components as

$$\begin{aligned} &\left[t_{ij} \left(u_s + u_s^{0} \right)_{,j} + \sigma_{ij} \left(\delta_{sj} + u_{s,j} + u_{s,j}^{0} \right) \right]_{,i} \\ &\quad + X_s^{0} + X_s + \Delta X_s - r \ddot{u}_s = 0 \\ &P_s^{0} + p_s + \Delta P_s = \left[t_{ij} \left(u_s + u_s^{0} \right)_{,j} + \sigma_{ij} \left(\delta_{sj} + u_{s,j} + u_{s,j}^{0} \right) \right] n_i \end{aligned} \tag{27}$$

where t_{ij}, u_s^{0}, X_s^{0}, and P_s^{0} stand for the initial stress, displacement, body force, and surface traction, respectively, and σ_{ij}, u_s, X_s, and p_s are the corresponding perturbation quantities. The terms ΔX_s and ΔP_s represent changes in the body force and surface traction due to perturbation.

Because the composite is in an equilibrium state before perturbation, the equation for incremental stresses and displacements can be reduced as follows:

$$\begin{aligned} &(t_{ij} u_s)_{,i} + \left[\sigma_{ij} \left(\delta_{sj} + u_{s,j} + u_{s,j}^{0} \right) \right]_{,i} + X_s + \Delta X_s - \rho \ddot{u}_s = 0 \\ &p_s + \Delta P_s = \left[t_{ij} u_{s,j} + \sigma_{ij} \left(\delta_{sj} + u_{s,j} + u_{s,j}^{0} \right) \right] n_i \end{aligned} \tag{28}$$

The equation of the virtual work can be obtained by multiplying Eq. (28) by the variation of the displacement component δu_s and then integrating the resulting expression over the volume D. Upon using the product differentiation rules and the divergence theorem, the equation becomes

$$\begin{aligned} &\delta (\bar{V} + \bar{W}) + \int_D \rho \ddot{u}_s \delta u_s \, \mathrm{d}v \\ &\quad = \int_s \left[t_{ij} u_{s,j} + \sigma_{is} + \sigma_{ij} \left(u_{s,j} + u_{s,j}^{0} \right) \right] \delta u_s n_i \, \mathrm{d}s \\ &\quad + \int_D (X_s + \Delta X_s) \delta u_s \, \mathrm{d}v \end{aligned} \tag{29}$$

where

$$\delta \bar{V} = \delta \int_D \frac{1}{2} \sigma_{ij} \varepsilon_{ij} \, \mathrm{d}v, \qquad \delta \bar{W} = \delta \int_D \frac{1}{2} t_{ij} u_{s,i} u_{s,j} \, \mathrm{d}v \tag{30}$$

The surface integral in Eq. (29) consists of the integration over the areas S_p and S_u in which surface tractions and displacements are prescribed, respectively. Therefore, from the second of Eqs. (28), the virtual work theorem is finally represented as

$$\begin{aligned} &\delta (\bar{V} + \bar{W}) + \int_D \rho \ddot{u}_s \delta u_s \, \mathrm{d}v = \int_{Sp} (p_s + \Delta P_s) \delta u_s \, \mathrm{d}s \\ &\quad + \int_{Su} \left[t_{ij} u_{s,j} + \sigma_{is} + \sigma_{ij} \left(u_{s,j} + u_{s,j}^{0} \right) \right] \delta u_s n_i \, \mathrm{d}s \\ &\quad + \int_D (X_s + \Delta X_s) \delta u_s \, \mathrm{d}v \end{aligned} \tag{31}$$

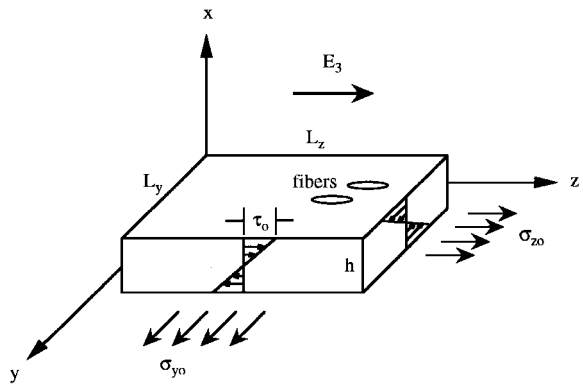

Fig. 2 Initial electromechanical stresses in the plate.

The tensor form of the virtual work theorem is valid for not only linear and conservative but also nonlinear and nonconservative problems. The equation will be used subsequently in deriving the equations of motion for arbitrarily prestressed plates.

Equation (31) is a general equation governing three-dimensional motion of the composite body. To illustrate the piezoelectic effect, the perturbing displacements in a plate composed of the short-fiber composite are examined. The plate is assumed to be rectangular with dimension L_y, L_z, and thickness h as shown in Fig. 2. The motion of the plate is assumed to be the following form[14,15]:

$$\begin{aligned} u_1(x, y, z, t) &= u(y, z, t) \\ u_2(x, y, z, t) &= v(y, z, t) + x\psi_y(y, z, t) \\ u_3(x, y, z, t) &= w(y, z, t) + x\psi_z(y, z, t) \end{aligned} \tag{32}$$

where u, v, and w are midplane displacements in the x, y, and z directions, respectively, and ψ_x and ψ_y are rotatory angles.

Based on the displacement functions, the strain can be expressed in terms of midplane strain and curvature vectors as

$$[\varepsilon(x, y, z, t)] = [\varepsilon_0(y, z, t)] + x[\kappa(y, z, t)] \tag{33}$$

where

$$\begin{aligned} [\varepsilon_0] &= [0, v_{,y}, w_{,z}, v_{,z} + w_{,y}, u_{,z} + \psi_z, u_{,y} + \psi_y]^T \\ [\kappa] &= [0, \psi_{y,y}, \psi_{z,z}, \psi_{y,z} + \psi_{z,y}, 0, 0]^T \end{aligned} \tag{34}$$

The force and moment resultants in the plate are defined as

$$\begin{aligned} [N_y, N_z, N_{yz}, N_{xz}, N_{xy}] &= \int_{-h/2}^{h/2} [\sigma_{yy}, \sigma_{zz}, \sigma_{yz}, \sigma_{xz}, \sigma_{xy}]^T \, dx \\ [M_y, M_z, M_{yz}, M_{xz}, M_{xy}] &= \int_{-h/2}^{h/2} x[\sigma_{yy}, \sigma_{zz}, \sigma_{yz}, \sigma_{xz}, \sigma_{xy}]^T \, dx \end{aligned} \tag{35}$$

The plate extensional and bending stiffnesses are defined as

$$A_{ij} = C_{ij}h, \qquad D_{ij} = C_{ij}(h^3/12) \tag{36}$$

where C_{ij} is the corresponding two-index matrix of the stiffness tensor C^c_{iJAb}.

Performing all of the integrations in Eq. (31), taking variations with respect to all variables, neglecting small terms, and collecting terms that contain variations of the same displacements, one obtains

$$\begin{aligned} &\int_0^{L_z}\int_0^{L_y} \{H_1\delta u + H_2\delta v + H_3\delta w + H_4\delta\psi_y + H_5\delta\psi_z\} \, dy \, dz \\ &+ \int_0^{L_y} [I_1\delta u + I_2\delta v + I_3\delta w + I_4\delta\psi_y + I_5\delta\psi_z]_{y=0}^{y=L_y} \, dy \\ &+ \int_0^{L_z} [J_1\delta u + J_2\delta v + J_3\delta w + J_4\delta\psi_y + J_5\delta\psi_z]_{z=0}^{z=L_z} \, dz = 0 \end{aligned} \tag{37}$$

where H_i, I_i, and J_i consist of the displacement functions [Eq. (32)], the stiffnesses [Eq. (36)], and the initial forces and moments. The details of H_i, I_i, and J_i are lengthy and are not listed here.

Initial stresses within the plate can be introduced from two sources: mechanical and electrical loadings. Because it has been assumed that the induced initial stresses are linear as defined in Eq. (1), the total initial stress can be represented by a single term. Although there are infinite combinations of the initial stresses, only the mechanical stresses σ_{y0}, σ_{z0}, and τ_0 and an electric field E_3 are discussed (Fig. 2). The resulting initial stresses can be expressed in the following forms:

$$t_{22} = \sigma_{y0} - e_{31}E_3, \qquad t_{33} = \sigma_{z0} - e_{33}E_3, \qquad t_{23} = (2x/h)\tau_0 \tag{38}$$

The terms σ_{y0}, σ_{z0}, τ_0, and E_3 are constants so that the initial stresses are uniform. The resultant forces and moments due to the initial stresses can be found as

$$\begin{aligned} (\bar{N}_y, \bar{N}_z) &= (t_{22}, t_{33})h, \qquad \bar{M}_{yz} = \tau_0(h^2/6) \\ (\bar{M}^*_y, \bar{M}^*_z) &= (t_{22}, t_{33})(h^3/12) \end{aligned} \tag{39}$$

If the plate is simply supported at the boundaries, the following displacement functions satisfying the boundary conditions are introduced:

$$\begin{aligned} u &= C_1 h \sin(\xi)\sin(\eta)\, e^{i\omega t}, \qquad v = C_2 h \sin(\xi)\cos(\eta)\, e^{i\omega t} \\ w &= C_3 h \cos(\xi)\sin(\eta)\, e^{i\omega t}, \qquad \psi_y = C_4 \cos(\xi)\sin(\eta)\, e^{i\omega t} \\ \psi_z &= C_5 \sin(\xi)\cos(\eta)\, e^{i\omega t} \end{aligned} \tag{40}$$

where $\xi = m\pi y/a$, $\eta = n\pi z/b$, and C_i, ω, and t are coefficients, frequency, and time, respectively. The plate characteristic equation can be found by substituting Eq. (40) into the equation of motion (37). A set of five homogeneous equations can be obtained as

$$K_{ij}C_j = 0, \qquad i, j = 1, \ldots, 5 \tag{41}$$

The terms K_{ij} are listed in the Appendix. For nonzero solutions to exist, the determinant of the coefficient matrix $[\boldsymbol{K}]$ must vanish, enabling us to evaluate the eigenvalues for plate stability and vibration under initial stresses.

Results and Discussion

In this paper, two composite systems are examined: $BaTiO_3$/PZT-5H and carbon/PZT- 5H. Both $BaTiO_3$ and PZT-5H are piezoelectric materials, and carbon is a typical reinforcing fiber with a high modulus along the axial direction. The electroelastic properties of these constituents are given as follows.[12]

$BaTiO_3$ fiber:

$$C^*_{11} = 166,\ C^*_{33} = 162,\ C^*_{44} = 43,\ C^*_{12} = 77,\ C^*_{13} = 78\,\text{GPa}$$

$$e^*_{31} = -4.4,\ e^*_{33} = 18.6,\ e^*_{15} = 11.6\,\text{C/m}^2$$

$$\kappa^*_{11} = 11.2 \times 10^{-9},\ \kappa^*_{33} = 12.6 \times 10^{-9}\,\text{C}^2/\text{Nm}^2$$

Carbon fiber:

$$C^*_{11} = 20,\ C^*_{33} = 390,\ C^*_{44} = 40,\ C^*_{12} = 8,\ C^*_{13} = 15\,\text{GPa}$$

PZT-5H matrix:

$$C^m_{11} = 126,\ C^m_{33} = 117,\ C^m_{44} = 35.3,\ C^m_{12} = 77,\ C^m_{13} = 55\,\text{GPa}$$

$$e^m_{31} = -6.5,\ e^m_{33} = 23.3,\ e^m_{15} = 17.0\,\text{C/m}^2$$

$$\kappa^m_{11} = 15.1 \times 10^{-9},\ \kappa^m_{33} = 13.0 \times 10^{-9}\,\text{C}^2/\text{Nm}^2$$

Based on the matrix material, the Eshelby tensors are first evaluated numerically from Eqs. (7) and (8) with various inclusion aspect ratios a_3/a_1. Note that the tensors are independent of inclusion

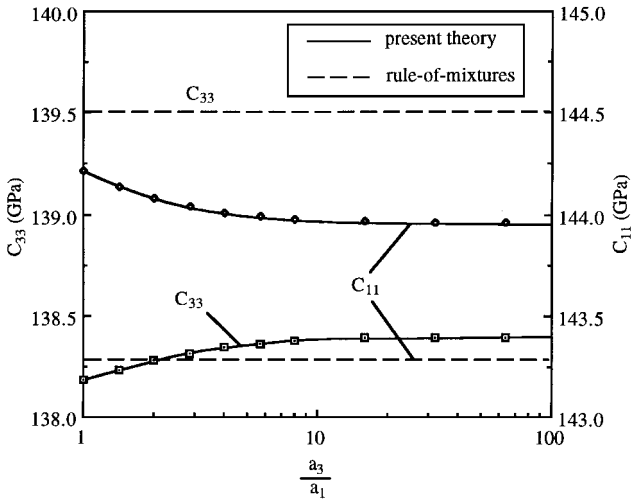

Fig. 3 Elastic moduli vs fiber aspect ratio of the $BaTiO_3$/PZT-5H composite ($f = 0.5$).

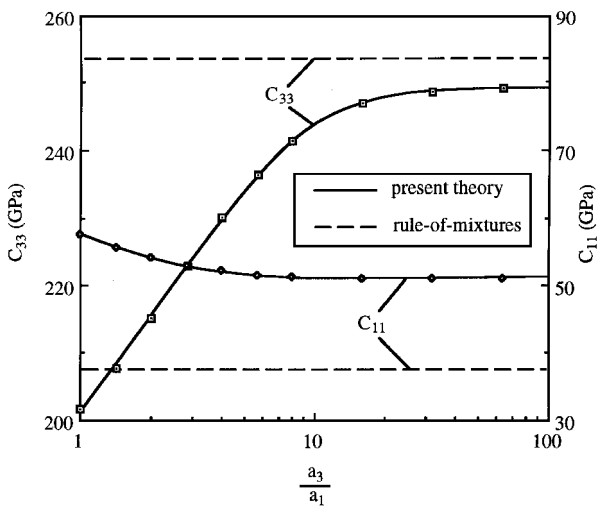

Fig. 4 Elastic moduli vs fiber aspect ratio of the carbon/PZT-5H composite ($f = 0.5$).

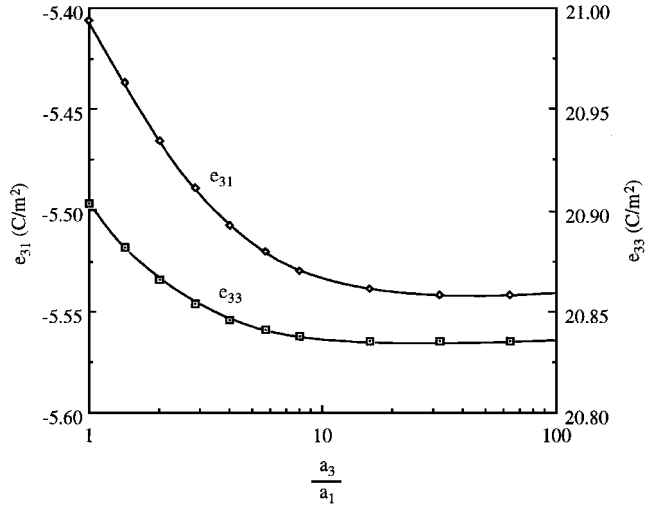

Fig. 5 Piezoelectric constants vs fiber aspect ratio of the $BaTiO_3$/PZT-5H composite ($f = 0.5$).

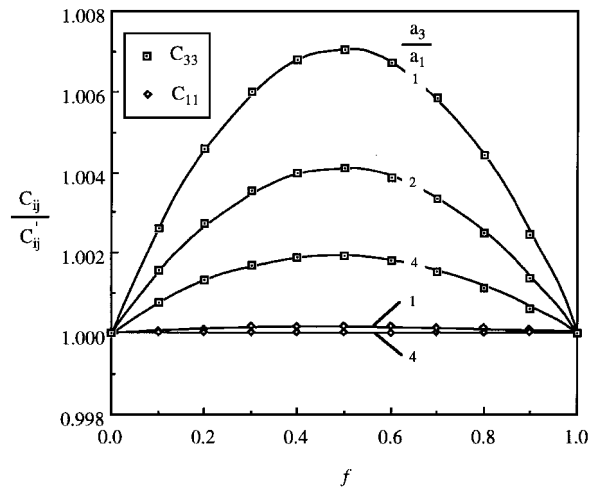

Fig. 6 Piezoelectric effects on the moduli of the $BaTiO_3$/PZT-5H composite (C'_{ij}: without piezoelastic coupling).

properties. Once the tensors are obtained, the effective properties of the composites can be calculated according to Eqs. (23) and (26).

Figure 3 shows the obtained moduli C_{11} and C_{33} for the $BaTiO_3$/PZT-5H composite. It can be seen that the modulus in the longitudinal direction C_{33} is increased when the fiber aspect ratio increases. In comparison, the modulus in the transverse direction C_{11} is decreased with the fiber aspect ratio. For this composite, the fiber aspect ratio only marginally affects the resulting moduli. For the carbon/PZT-5H system, however, the aspect ratio is found to significantly affect the axial modulus as shown in Fig. 4 because the carbon fiber is a highly nonisotropic material. Also shown in the figures are corresponding results from the simple rule-of-mixtures approach based on an isostrain assumption for C_{33} and an isostress assumption for C_{11}. This widely used model provides an easy approximation for composite moduli. However, the simplified assumptions ignore the influence of fiber shapes. Thus, the results are independent of the fiber aspect ratio. According to the figures, the difference between the rule-of-mixtures approach and the present micromechanics approach is more pronounced when fibers are shorter. Despite this inherent limitation, the elastic constants predicted by the present theory and the rule-of-mixtures approach differ less than 1% for the $BaTiO_3$/PZT-5H system. One reason is that the moduli of the $BaTiO_3$ fiber and PZT-5H matrix are relatively close. Thus, the effect of strain concentration on composite elastic behavior due to inclusion shape and material discontinuity is relatively insubstantial for this material system. In comparison, the difference is more than 25% for C_{33} of the carbon/PZT-5H system when $a_3/a_1 = 1$. When the aspect ratio becomes greater (>10 for the cases studied), the moduli approach their asymptotic values, indicating that the reinforcing effect due to fiber length is saturated beyond this value. The resulting piezoelectric constants e_{31} and e_{33} for the $BaTiO_3$/PZT-5H composite are shown in Fig. 5. When the aspect ratio increases, e_{33} is decreased, whereas the absolute value of e_{31} is increased.

Effects of piezoelastic coupling on the composite moduli are also studied. To this end, the moduli are compared with the corresponding results by assuming that all piezoelectric constants vanish, i.e., $e_{imn} = 0$. The results in the absence of piezoelectric coupling are denoted as C'_{ij}. The ratios between C_{ij} and C'_{ij} are plotted in Figs. 6 and 7 with varying fiber volume fraction and aspect ratio. For the $BaTiO_3$/PZT-5H composite, all independent elastic moduli (C_{11}, C_{33}, C_{12}, C_{13}, and C_{66}) are higher than the corresponding values of C'_{ij}. Among the five moduli, it is found that C_{33} is more affected by the piezoelectric effect than the others. For the carbon/PZT-5H composite, C_{13} is decreased due to the presence of piezoelastic coupling, whereas the others are increased. It is found that the piezoelectric effect is more significant when fibers are shorter. When $f = 0$ and 1, the composite becomes monolithic, and the piezoelectric coupling effect vanishes. The maximum effect occurs at about $f = 0.5$ for the $BaTiO_3$/PZT-5H composite and $f = 0.6$ for the carbon/PZT-5H composite.

The fundamental frequencies of the plate under initial electromechanical loading are obtained from Eq. (41). To simplify the discussion, plate dimensions with $L_y/h = 10$ and $L_z/h = 10$ are used. Figure 8 shows the results for the carbon/PZT-5H composite under initial normal stresses σ_{y0} and σ_{z0}. It is seen that the fundamental

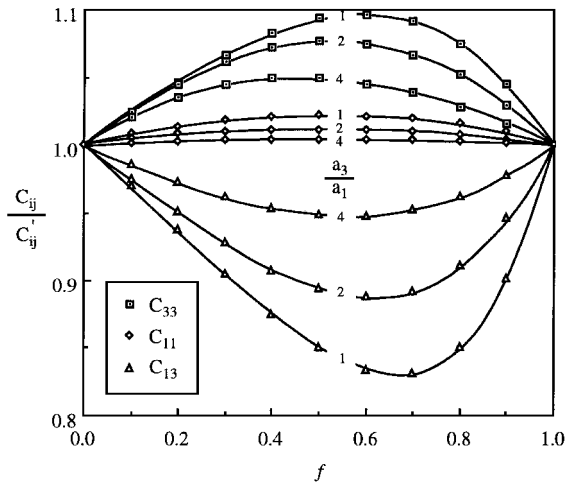

Fig. 7 Piezoelectric effects on the moduli of the carbon/PZT-5H composite (C'_{ij}: without piezoelastic coupling).

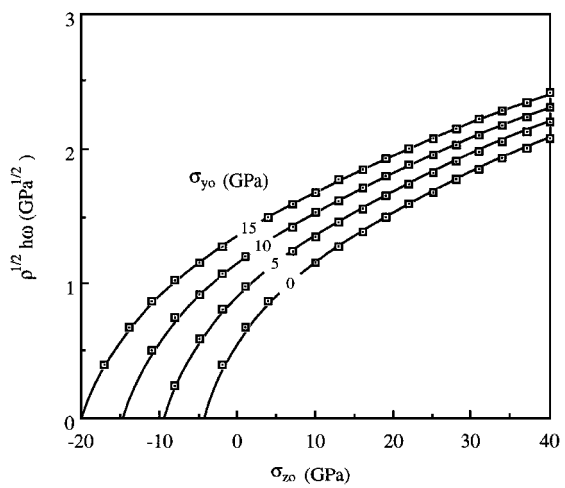

Fig. 8 Fundamental frequencies of the carbon/PZT-5H plate under σ_{y0} and σ_{z0} ($a_3/a_1 = 2$ and $f = 0.5$).

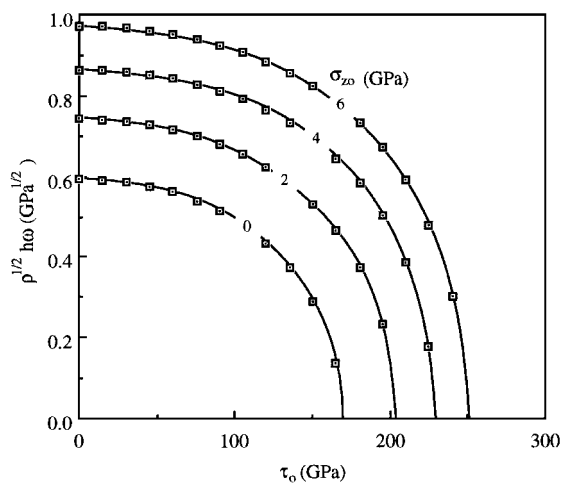

Fig. 9 Fundamental frequencies of the carbon/PZT-5H plate under τ_0 and σ_{z0} ($a_3/a_1 = 2$ and $f = 0.5$).

frequencies are increased when either σ_{y0} or σ_{z0} is increased; this is simply due to plate tensioning. When both σ_{y0} and σ_{z0} are zero, the point refers to the natural frequency. As σ_{z0} becomes negative, the fundamental frequency will eventually vanish as the compressive stress increases; the zero frequency can be defined as buckling of the plate. Higher compressive stress is required to buckle the plate if the tensile stress in the other direction (σ_{y0}) increases. Figure 9 illustrates the effect of initial shear stresses on the plate. As τ_0 increases, the fundamental frequencies are reduced and will eventually vanish

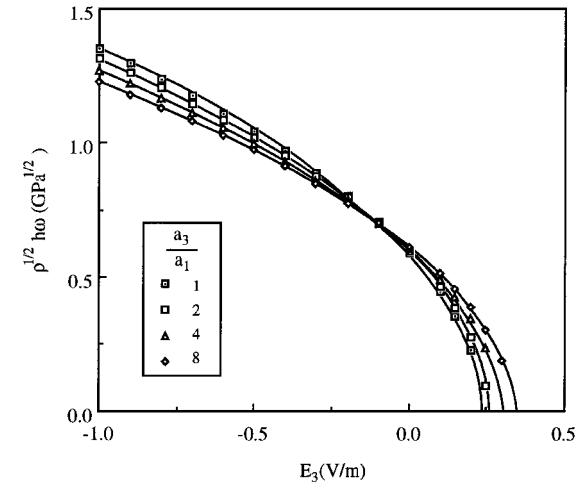

Fig. 10 Fundamental frequencies of the carbon/PZT-5H plate under E_3 ($f = 0.5$).

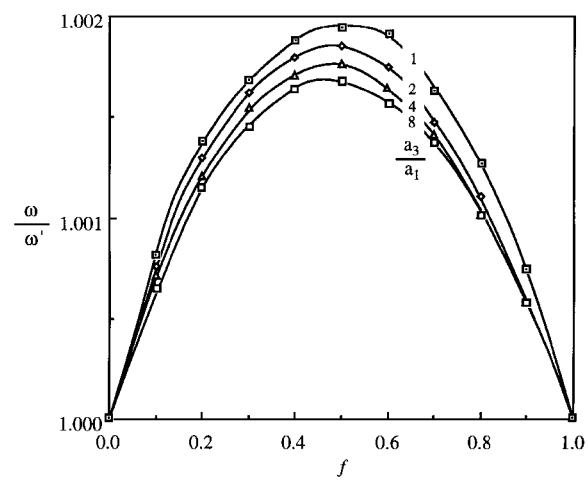

Fig. 11 Piezoelectric coupling effects on natural frequencies of the $BaTiO_3$/PZT-5H plate (ω': without piezoelastic coupling).

when plate buckling due to the initial shear stress occurs. Unlike the normal stresses, positive and negative shear stresses yield the same results for fundamental frequencies and buckling loads. Because the composite is piezoelectric, applying an electric field also induces initial stresses. Figure 10 shows the frequencies as functions of the electric field E_3. When a positive E_3 is applied, a smaller positive σ_{y0} and a larger negative σ_{z0} are induced simultaneously according to the constitutive relation [Eq. (1)] and the obtained composite e_{ij} values. Thus, the negative σ_{z0} is the dominant stress for plate vibration. As E_3 increases, the plate is subjected to compressive stress, and the frequencies are reduced. Plate buckling will occur once the applied electric field reaches a critical level. The fiber aspect ratio affects the resulting piezoelectric constants and the frequency as well. Note that the results in the figures are the lowest eigenvalues searched, and the corresponding mode is $m = n = 1$; it is possible that the lowest results can occur in other modes if the plate dimensions or material constants are changed. Note that when applying initial loads other than forces, such as electric fields and hygrothermal loads, the displacements at the boundaries of the plate should be constrained so that the initial normal stresses can be induced.

The piezoelectric effects on natural frequencies of the plate are shown in Figs. 11 and 12. Likewise, the corresponding results (ω') in the absence of piezoelectric coupling are used to evaluate the effects. Because natural frequency is a function of elastic moduli, the piezoelectric effects on the frequency must be closely related to the effects shown in Figs. 5 and 6. Among the five elastic moduli, the in-plane normal ones (C_{11} and C_{33}) are dominant terms, whereas the in-plane shear (C_{13}) and transverse ones (C_{12} and C_{66}) are less influential unless the plate is very thick. Thus, piezoelectric effects on the frequency can be directly assessed based on the effects on C_{11} and C_{33}. Because both C_{11} and C_{33} are increased with the presence

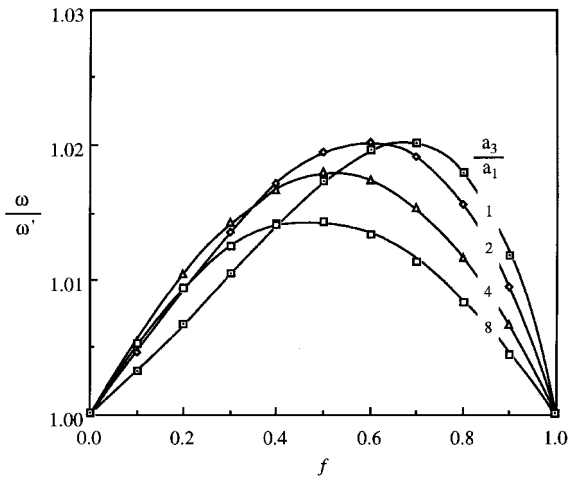

Fig. 12 Piezoelectric coupling effects on natural frequencies of the carbon/PZT-5H plate (ω' : without piezoelastic coupling).

of piezoelastic coupling, the same effects must also be seen in the frequency as revealed in Figs. 11 and 12. Similar to the effects on the moduli, the piezoelectric effects on the frequency vanish when the material becomes monolithic, and using shorter fibers generally results in higher coupling effects.

Conclusion

In this paper, two approaches have been used to analyze the dynamic response of the short-fiber plates. One is the micromechanics method aimed at finding the effective piezoelastic constants of the composite. Through the use of the Mori–Tanaka mean field theory and piezoelectric Eshelby tensors, the effect of geometric shape of inclusions has been assessed. The other is the variational principle using the Trefftz stress components to take into account initial stresses. With the principle, the general equations of motion can be obtained. No terms are dropped unnecessarily, and the equation derived here can be used to assess postbuckling and large deformation problems as well as nonconservative stability and dynamic behavior for various states of initial loads. Numerical examinations for two composite systems have been given. Because of the highly anisotropic behavior of the carbon fiber, fiber aspect ratio is found to be more influential in the carbon/PZT-5H than in the $BaTiO_3$/PZT-5H system. For both systems, piezoelastic coupling provides a stiffening effect, which is more pronounced for the carbon/PZT-5H system. The results indicate that the longitudinal modulus and in-plane shear modulus are increased with the fiber aspect ratio and the piezoelectric and dielectric constants are decreased with the ratio. Consequently, the composite natural frequency and buckling stresses are increased due to the presence of piezoelectric effects. When the fiber volume fraction approaches 0 or 1, the stiffening effect disappears. The results by the rule-of-mixtures approach have been compared with the present analysis, and the limitation of the rule has been discussed. Besides the stiffening effects, piezoelastic coupling can also affect the fundamental frequency through initial electric loadings, which can induce a combination of initial normal and shear stresses dependent on the resulting composite piezoelectric properties.

Appendix: Coefficients

The coefficients in Eq. (41) are given as follows:

$$K_{11} = C_{66}\lambda_y^2 + C_{55}\lambda_z^2 - \rho h^2\omega^2 + \sigma_{y0}\lambda_y^2 + \sigma_{z0}\lambda_z^2$$

$$K_{14} = C_{66}\lambda_y, \qquad K_{15} = C_{55}\lambda_z$$

$$K_{22} = C_{22}\lambda_y^2 + C_{44}\lambda_z^2 - \rho h^2\omega^2 + \sigma_{y0}\lambda_y^2 + \sigma_{z0}\lambda_z^2$$

$$K_{23} = (C_{23} + C_{44})\lambda_y\lambda_z, \qquad K_{24} = \tfrac{1}{3}\tau_0\lambda_y\lambda_z$$

$$K_{33} = C_{33}\lambda_z^2 + C_{44}\lambda_y^2 - \rho h^2\omega^2 + \sigma_{y0}\lambda_y^2 + \sigma_{z0}\lambda_z^2$$

$$K_{35} = \tfrac{1}{3}\tau_0\lambda_y\lambda_z$$

$$K_{44} = C_{66} + \tfrac{1}{12}C_{22}\lambda_y^2 + \tfrac{1}{12}C_{44}\lambda_z^2 - \tfrac{1}{12}\rho h^2\omega^2 + \tfrac{1}{12}\sigma_{y0}\lambda_y^2 + \tfrac{1}{12}\sigma_{z0}\lambda_z^2$$

$$K_{45} = \tfrac{1}{12}(C_{23} + C_{44})\lambda_y\lambda_z$$

$$K_{55} = C_{55} + \tfrac{1}{12}C_{33}\lambda_z^2 + \tfrac{1}{12}C_{44}\lambda_y^2 - \tfrac{1}{12}\rho h^2\omega^2 + \tfrac{1}{12}\sigma_{y0}\lambda_y^2 + \tfrac{1}{12}\sigma_{z0}\lambda_z^2$$

where $\lambda_y = m\pi h/L_y$ and $\lambda_z = n\pi h/L_z$.

Acknowledgment

The author wishes to thank the National Science Council of Taiwan, Republic of China, for the support of this research (NSC 86-2216-E-035-014).

References

[1] Kuo, W. S., and Huang, J. H., "Stability and Vibration of Initially Stressed Plates Composed of Spatially Distributed Fiber Composites," *Journal of Sound and Vibration*, Vol. 199, No. 1, 1997, pp. 51–69.

[2] Christensen, R. M., and Waals, F. M., "Effective Stiffness of Randomly Oriented Fibre Composites," *Journal of Composite Materials*, Vol. 6, 1972, pp. 518–532.

[3] Halpin, J. C., Jerine, K., and Whitney, J. M., "The Laminate Analogy for 2 and 3 Dimensional Composite Materials," *Journal of Composite Materials*, Vol. 5, 1971, pp. 36–49.

[4] Kuo, W. S., and Chou, T. W., "Multiple Cracking of Unidirectional and Cross-Ply Ceramic Matrix Composites," *Journal of the American Ceramic Society*, Vol. 78, No. 3, 1995, pp. 745–755.

[5] Aveston, J., and Kelly, A., "Theory of Multiple Fracture of Fibrous Composites," *Journal of Materials Science*, Vol. 8, 1973, pp. 352–362.

[6] Eshelby, J. D., "The Determination of the Elastic Field of an Ellipsoidal Inclusion and Related Problems," *Proceedings of the Royal Society*, Vol. A241, 1957, pp. 376–396.

[7] Mori, T., and Tanaka, K., "Average Stress in Matrix and Average Energy of Materials with Misfitting Inclusion," *Acta Metallurgica*, Vol. 21, 1973, pp. 571–574.

[8] Mura, T., *Micromechanics of Defects in Solids*, Martinus–Nijhoff, Dordrecht, The Netherlands, 1987, p. 74.

[9] Benveniste, Y., "On the Micromechanics of Fibrous Piezoelectric Composites," *Mechanics of Materials*, Vol. 18, No. 3, 1994, pp. 183–193.

[10] Weng, G. J., and Phillips, A., "The Stress Fields of Continuous Distribution of Dislocations and of Their Movement in a Polycrystalline Aggregate," *International Journal of Solids and Structures*, Vol. 14, 1978, pp. 535–544.

[11] Dunn, M. L., and Taya, M., "Micromechanics Predictions of the Effective Electroelastic Moduli of Piezoelectric Composites," *International Journal of Solids and Structures*, Vol. 30, No. 2, 1993, pp. 161–175.

[12] Kuo, W. S., and Huang, J. H., "On the Electroelastic Properties of the Composites Composed of Spatially Oriented Inclusions and Piezoelectric Matrix," *International Journal of Solid and Structures*, Vol. 34, No. 19, 1997, pp. 2445–2461.

[13] Bolotin, V. V., *Non-Conservative Problems of the Theory of Elastic Stability*, Macmillan, New York, 1963, Chap. 1.

[14] Kuo, W. S., and Yang, I. H., "Generic Nonlinear Behavior of Antisymmetric Angle-Ply Laminated Plates," *International Journal of Mechanical Science*, Vol. 31, No. 2, 1989, pp. 131–143.

[15] Yang, I. H., and Kuo, W. S., "Stability and Vibration of Initially Stressed Thick Laminated Plates," *Journal of Sound and Vibration*, Vol. 168, No. 2, 1993, pp. 285–297.

R. K. Kapania
Associate Editor